Journal of the Geological Society, London, Vol. **163**, 2006, pp. 983–995. Printed in Great Britain.

Provenance of late Palaeozoic metasediments of the SW South American Gondwana margin: a combined U–Pb and Hf-isotope study of single detrital zircons

CARITA AUGUSTSSON[1,2], CARSTEN MÜNKER[2,3], HEINRICH BAHLBURG[1] & C. MARK FANNING[4]

[1]*Geologisch–Paläontologisches Institut, Westfälische Wilhelms-Universität, Corrensstrasse 24, 48149 Münster, Germany (e-mail: augustss@uni-muenster.de)*

[2]*Zentrallaboratorium für Geochronologie, Institut für Mineralogie, Westfälische Wilhelms-Universität, Corrensstrasse 24, 48149 Münster, Germany*

[3]*Mineralogisch–Petrologisches Institut, Universität Bonn, Poppelsdorfer Schloss, 53115 Bonn, Germany*

[4]*Research School of Earth Sciences, The Australian National University, Mills Road, Canberra, A.C.T. 0200, Australia*

Abstract: Combined U–Pb and Lu–Hf isotope measurements of single detrital zircon grains in Carboniferous metasediments from Patagonia delineate the source areas of the sediments. The detritus, represented by four metasandstone samples, was deposited prior to onset of subduction in Late Carboniferous time along the south Patagonian proto-Pacific Gondwana margin. A broad series of detrital zircon age peaks (0.35–0.7 Ga, 0.9–1.5 Ga) and a large spread (0.3–3.5 Ga) in the age spectra require numerous sources. A fifth metasediment was deposited after the onset of subduction. This syncollisional sample shows two distinct U–Pb age peaks at *c*. 290 Ma and 305 Ma. This points to a few sources only (Patagonia, West Antarctica). Initial Hf-isotope compositions of selected U–Pb dated zircons from the Carboniferous metasediments reveal zircon protoliths originating from both recycled crust and juvenile sources ($\varepsilon Hf_{(T=0.4–3.5Ga)} = -14$ to +12). A comparison with crustal compositions of possible source areas indicates that the detritus mainly originated from the interior of Gondwana (Extra-Andean Patagonia, the Argentine Sierra de la Ventana, southernmost Africa, East Antarctica), as well as northern Chile and northwestern Argentina. The sediment transportation paths are consistent with an autochthonous palaeogeographical position of Patagonia with respect to Gondwana in Carboniferous time.

The initial Hf-isotope composition of single detrital zircon grains of known age is a powerful tool in provenance studies, particularly for cases where several potential source areas with similar zircon crystallization ages exist (Amelin *et al*. 1999; Bodet & Schärer 2000). Previous studies have demonstrated the potential of Hf-isotope measurements of single detrital zircons to address problems related to crustal evolution and terrane studies (e.g. Patchett 1983; Amelin *et al*. 1999, 2000; Bodet & Schärer 2000; Knudsen *et al*. 2001; Samson *et al*. 2003). In the past decade developments in instrumentation (multicollector inductively coupled plasma mass spectrometry; MC-ICPMS) have facilitated Hf-isotope measurements of single zircon grains as small as 50 μm with high precision and accuracy (e.g. Amelin *et al*. 2000; Blichert-Toft 2001; Nebel-Jacobsen *et al*. 2005). This is of considerable importance in provenance studies as detrital zircons typically are <100 μm in size.

The origin of Patagonia has been widely debated following the contention of Ramos (1984) that Patagonia might be an allochthonous continental fragment that collided with Gondwana in Carboniferous to Permian or Triassic time. Despite a number of investigations, both supporting (e.g. Dalziel & Grunow 1992; von Gosen 2003; Chernicoff & Zappettini 2004) and refuting (e.g. Varela *et al*. 1991; Rapalini 1998; Pankhurst *et al*. 2003) the concept of an exotic origin of the terrane, the plate-tectonic history of Patagonia is still controversial.

In this study, we present new sensitive high-resolution ion microprobe (SHRIMP) U–Pb ages and Hf-isotope data from single detrital zircons in metaturbiditic deposits of ?Carboniferous to Early Permian age from the metasedimentary basement of the southern Patagonian Andes, Chile and Argentina. The initial Hf-isotope compositions of the zircons are compared with previously published initial Nd-isotope compositions from possible source areas in southern Gondwana, of which most are dominated by rocks of similar crystallization ages. Based on our combined U–Pb and Lu–Hf approach, sedimentary transportation paths, with implications for the origin and tectonic evolution of Patagonia, are presented.

Tectonic and geological setting

In late Palaeozoic to early Mesozoic time, the proto-Pacific was subducted beneath the Patagonian margin of Gondwana. Andean Patagonia (Chile and western Argentina south of *c*. 42°S) was suggested to be part of a forearc province (Forsythe 1982). In northern Chilean Patagonia, Rb–Sr mineral isochron ages (296.6 ± 4.7 Ma, 305.3 ± 3.2 Ma, apatite, quartz + feldspar, white mica from a mica-schist; apatite, titanite, epidote, white mica from an amphibolite; Willner *et al*. 2004*a*) at Los Pabilos (*c*. 41°S) indicate that the onset of subduction occurred no later than *c*. 300 Ma. In central Chile the onset of subduction might have been somewhat earlier, as indicated by *c*. 320 Ma metamorphic Ar–Ar ages of phengite in garnet mica-schists at Pichilemu (*c*. 34°30′S; 317.8 ± 1.1 Ma, 319.5 ± 1.4 Ma; Willner *et al*. 2005). In southern Patagonia, zircon fission-track ages in

metasandstones support metamorphism at *c*. 250 Ma (Thomson & Hervé 2002).

The Patagonian Palaeozoic metasedimentary rocks, mainly siliciclastic metaturbidites, are the oldest exposed rocks in southern Andean Patagonia, with biostratigraphic ages from Devonian to Triassic (Fig. 1; Riccardi 1971; Douglass & Nestell 1976; Ling *et al*. 1985; Ling & Forsythe 1987; Fortey *et al*. 1992; Fang *et al*. 1998). The sediments were incorporated into subduction complexes that were accreted to the margin of Gondwana in late Palaeozoic to late Mesozoic time (zircon fission-track ages between 142 ± 7 Ma and 270 ± 17 Ma from metasandstones, K–Ar age of 117 ± 28 Ma from amphibolite; Thomson & Hervé 2002; Willner *et al*. 2004*b*). The western part of the deposits was incorporated into an accretionary wedge, and the eastern part into the backstop of the wedge. This resulted in deformation and metamorphism. The metamorphic grade of the metasediments varies from sub-greenschist to greenschist facies in the east to greenschist facies in the west (Willner *et al*. 2000; Ramírez-Sánchez *et al*. 2005). The metasediments were further subjected to large-scale deformation and folding in Late Cretaceous to Cenozoic time during development of the Andes (Ramos 1989).

The metasediments in this study are part of the low-grade Eastern Andean Metamorphic Complex in the east. They were sampled from the Argentine Bahía de la Lancha Formation and

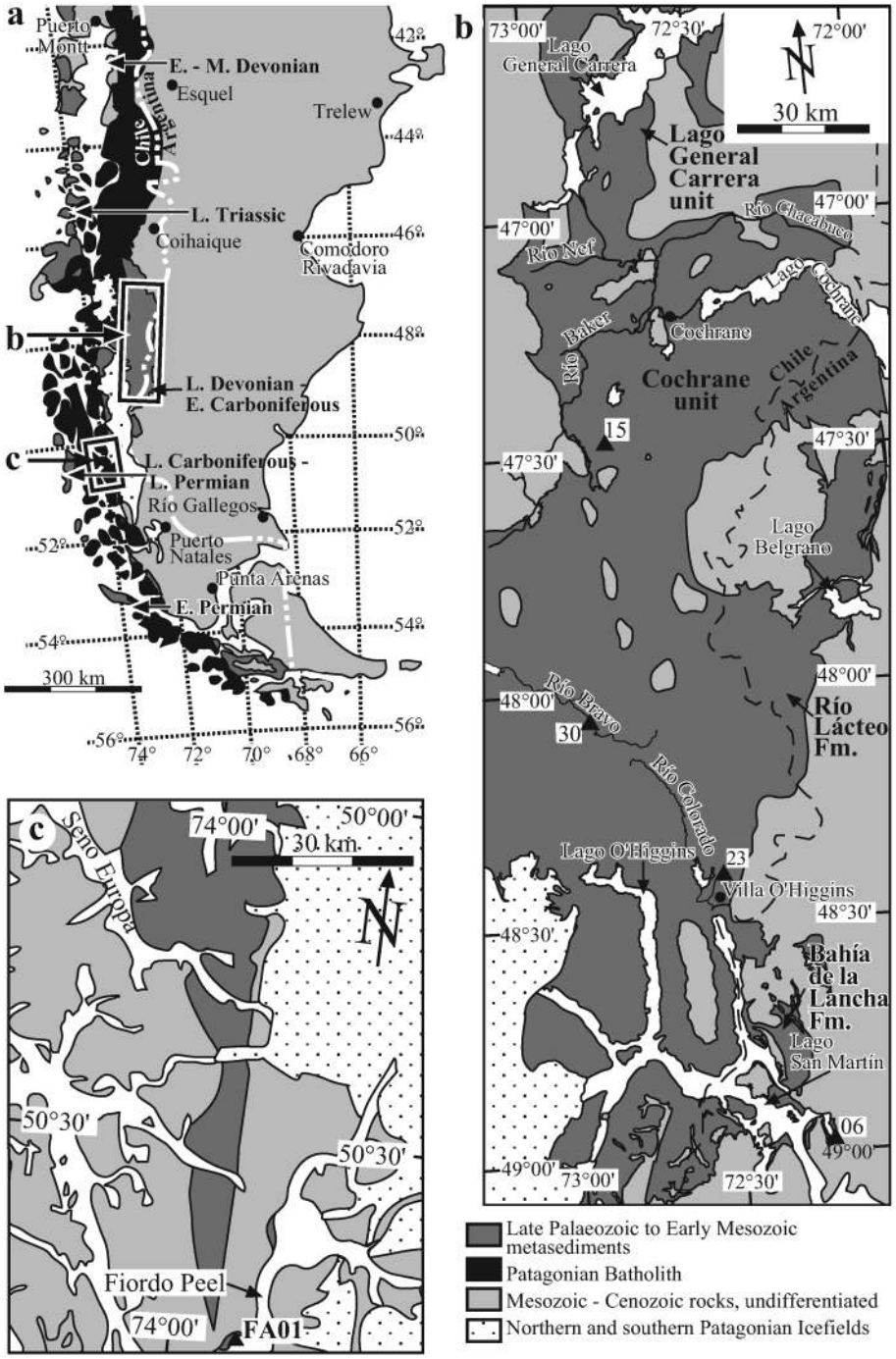

Fig. 1. (**a**) Map of southern Patagonia with age estimates of the Andean basement rocks determined from fossils. (For references, see text.) (**b**) and (**c**) show sampling areas. ▲, sampling points. Maps compiled from Nullo *et al*. (1978), Escobar (1980), Giacosa (1999) and Augustsson & Bahlburg (2003).

the Chilean Cochrane unit (northeastern Eastern Andean Metamorphic Complex), as well as from a more southwestern section of the Eastern Andean Metamorphic Complex in the Chilean Archipelago (Table 1, Fig. 1). The metasediments studied are thin-bedded sandstone-dominated metaturbidites. Mineralogically, they are dominated by quartz grains, and to a minor degree by plagioclase, in a clay-size matrix. Lithic fragments are scarce and are always of sedimentary origin. The metasediments display a felsic bulk composition with trace element and Nd-isotope ratios ($\epsilon Nd_{(T=280–350Ma)}$ of −7 to −5) that indicate an upper continental crustal origin for the major part of the detritus (Augustsson & Bahlburg 2003; Augustsson *et al*. 2004).

The Late Devonian to Early Carboniferous biostratigraphic age of metasandstones of the Argentine Bahía de la Lancha Formation close to the Chilean border (Riccardi 1971) is commonly adopted for a large part of the Eastern Andean Metamorphic Complex. However, U–Pb and fission-track ages of detrital zircons (Thomson & Hervé 2002; Hervé *et al*. 2003; this study), which give estimates of maximum and minimum depositional ages, respectively, indicate a more complex history for the Patagonian units (see Fig. 2).

Analytical methods

Zircons from five metasediments were dated by the U–Pb method with SHRIMP-RG and SHRIMP I at the Research School of Earth Sciences, Australian National University, Canberra. After sieving, the heavy mineral fraction of the <250 μm fraction was separated with diiodinemethane. A random selection of the total zircon fraction was mounted in epoxy together with the FC1 and SL13 reference zircons (Paces & Miller 1993; Claoué-Long *et al*. 1995) and polished to expose the centres of the grains. Morphology and size were ignored when selecting mounted grains for analysis, to minimize a bias in the age spectra results. Zircon regions suitable for analysis were identified from cathodoluminescence (CL) imaging.

From each sample, 60–70 single detrital zircons were analysed following the method described by Williams (1998, and references therein). Zircon rims were preferentially analysed, to date the last growth stage of each zircon. Spot size was <30 μm. The U and Pb isotope data

Table 1. *Sampling locations of the metasandstones*

Sample	Geological unit	Coordinates
CA-00-15	Cochrane unit, northeastern Eastern Andean Metamorphic Complex, Chile	47°30′25.5″S, 72°50′18.0″W
CA-00-23	Cochrane unit, northeastern Eastern Andean Metamorphic Complex, Chile	48°24′58.1″S, 72°32′46.9″W
CA-00-30	Cochrane unit, northeastern Eastern Andean Metamorphic Complex, Chile	48°06′40.7″S, 72°55′28.6″W
CA-01-06	Bahía de la Lancha Fm, northeastern Eastern Andean Metamorphic Complex, Argentina	48°58′30.2″S, 72°13′46.7″W
FA-01	Southwestern Eastern Andean Metamorphic Complex, Chile	50°48′8.3″S, 73°52′56.8″W

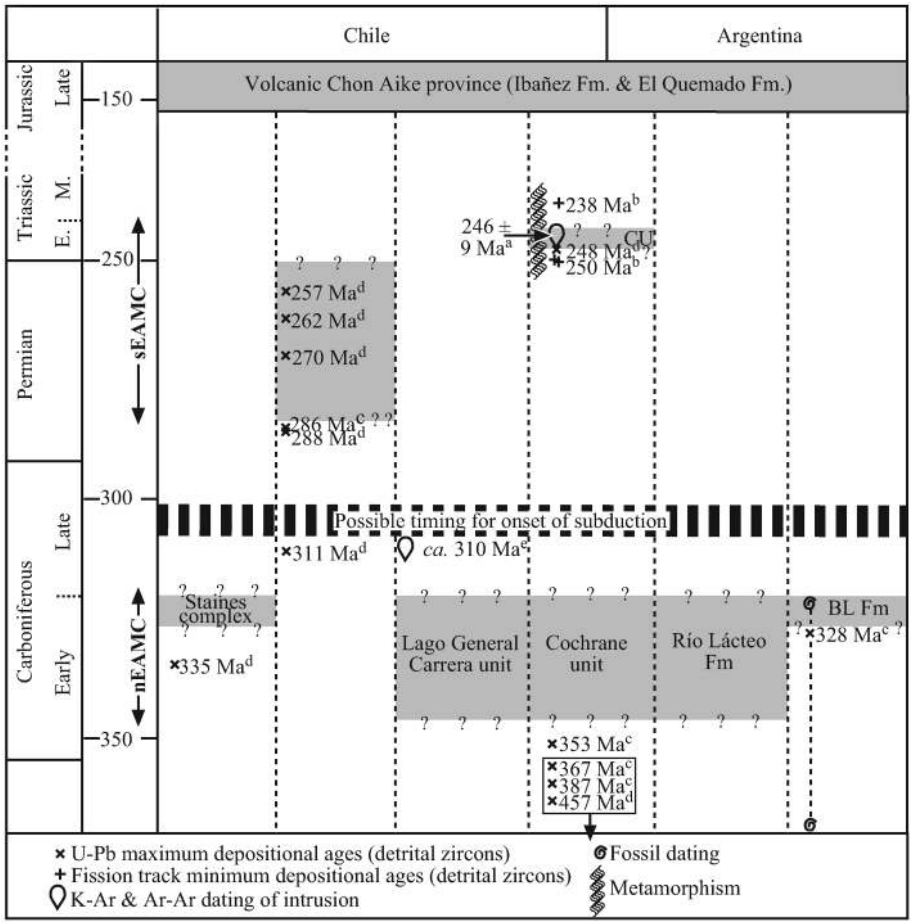

Fig. 2. Stratigraphy of the Eastern Andean Metamorphic Complex (EAMC). BL Fm, Bahía de la Lancha Formation; CU, Cochrane unit (with two possible sedimentary phases); nEAMC, northeastern EAMC; sEAMC, southwestern EAMC. The marked felsic plutonic rocks intruded the Eastern Andean Metamorphic Complex. The lower and upper age limits of the Eastern Andean Metamorphic Complex are uncertain. It should be noted that the radiometric ages are not actual depositional ages. The maximum depositional ages are based on the youngest dated concordant zircon in each sample, because the youngest reliable age peak commonly is much older than several younger grains. The timing for onset of subduction is based on results from southern Patagonia in this study and on Rb–Sr mineral dating (results from northern Patagonia; Willner *et al*. 2004*a*). The biostratigraphic dating is from Riccardi (1971). Sources of isotope ages: [a]Yoshida (1981); [b]Thomson & Hervé (2002); [c]this study; [d]Hervé *et al*. (2003)[e]; de la Cruz (pers. comm.).

consist of four scans through the mass spectrum. They were reduced with a procedure similar to that described by Williams (1998, and references therein) and with the SQUID/Ex Macro of Ludwig (2001*a*). The Pb/U values were normalized relative to $^{206}Pb/^{238}U = 0.1859$ of the FC1 reference zircons, equivalent to an age of 1099 Ma (see Paces & Miller 1993). For zircons older than *c*. 800 Ma, $^{207}Pb/^{206}Pb$ values were used for age calculation. Because of the small variability of $^{207}Pb/^{206}Pb$ in the Phanerozoic age range, $^{206}Pb/^{238}U$ ages were generally preferred for younger zircons. The $^{207}Pb/^{206}Pb$ ages were corrected for common Pb (with assumed present-day compositions of $^{206}Pb/^{204}Pb = 18.824$ and $^{207}Pb/^{204}Pb = 15.671$; Cumming & Richards 1975) based on ^{204}Pb, whereas $^{206}Pb/^{238}U$ ages were corrected based on ^{207}Pb as outlined by Williams (1998). Isoplot/Ex (Ludwig 2001*b*) was used for age calculations (assuming $\lambda(^{238}U) = 1.551 \times 10^{-10}a^{-1}$ and $\lambda(^{235}U) = 9.849 \times 10^{-10}a^{-1}$; Jaffey *et al*. 1971) and statistical treatment.

Seventeen zircons from sample CA-00-30 and seven zircons from CA-01-06 were analysed for their Lu and Hf concentrations and Hf-isotope compositions at the Zentrallaboratorium für Geochronologie Münster. After removal of the zircons from the epoxy, where they were embedded for the U–Pb dating, and prior to digestion, they were spiked with a mixed $^{176}Lu/^{180}Hf$ tracer. The dissolution procedure included a first step with 5:1 HF–HNO_3 in Teflon® bombs at 175 °C for 4 days. For Lu–Hf separation, the element separation method of Nebel-Jacobsen *et al*. (2005) was used. Lu and Hf measurements were performed by MC-ICPMS using a Micromass Isoprobe system. The operation conditions followed those described by Münker *et al*. (2001). Average $^{176}Hf/^{177}Hf$ values for the Münster AMES Hf standard (isotopically indistinguishable from JMC 475) on the three measurement days were 0.282146 ± 10, 0.282146 ± 12 and $0.282151 \pm \pm 14$ (errors are absolute $2\sigma \times 10^{-6}$). All data are given relative to $^{176}Hf/^{177}Hf = 0.282160$ for JMC 475. Laboratory Lu and Hf blanks were <1 pg and <10 pg, respectively, and are negligible for determinations of the initial Hf-isotope ratio. Blank corrections for Lu were always <5%. The mean external reproducibility is ±0.5 εHf-units (2σ). The epoxy (from Epirez Construction Products, Australia), in which the zircons were embedded, was analysed for its Lu–Hf content (<0.5 pg Lu and 0.5 pg Hf in >125 000 μm^3 epoxy) to ensure that the epoxy residue did not affect the zircon analyses.

U–Pb ages

U–Pb ages were determined for a total of 300 zircon spots with only one growth phase. In the four analysed northeastern Eastern Andean Metamorphic Complex samples (CA-00-15, -23, -30 from the Cochrane unit, and CA-01-06 from the Bahía de la Lancha Formation), the dated zircons are typically 50–150 μm in length and sub-round to round in shape (see Fig. 3). Of the 239 dated zircons in these samples, 56% display oscillatory and/or sector zoning, interpreted as magmatic zoning, whereas 44% display metamorphic zoning (rounded concentric or irregular zoning, or unzoned), as revealed by CL images (Fig. 3). The U–Pb age spectra of the four samples are dominated by a broad series of age peaks in the range from 350 to 700 Ma (Figs 4 and 5). Minor age peaks are apparent at 0.9–1.5 Ga. Of the zircons, 90% have ages <1.5 Ga. Only 5% are of Archaean age (Fig. 4). The U–Pb age of the youngest concordant grain (Fig. 5) in each of the four samples is between 320 and 390 Ma, pointing to maximum depositional ages between *c*. 330 and 385 Ma (considering their 1σ errors; latest Mid-Devonian to latest Early Carboniferous). The youngest age (323 ± 5 Ma;) is exhibited by the Argentine Bahía de la Lancha Formation, earlier dated as Late Devonian to Early Carboniferous (Riccardi 1971).

The zircons in the fifth sample (FA-01 from the southwestern Eastern Andean Metamorphic Complex) are typically euhedral, elongated grains 100–200 μm in length (see Fig. 3). Of the 61 analysed spots with a single growth phase, 84% have magmatic zoning, whereas 16% have metamorphic zoning (Figs 3–5). The oldest dated zircon in this sample is 2.2 Ga in age, and 84% have ages <500 Ma (Fig. 4). Major distinct age peaks occur at *c*. 290 Ma and *c*. 305 Ma (Fig. 4). The maximum depositional age can be constrained to *c*. 285 Ma (Early Permian) given by the youngest concordant age at 282 ± 4 Ma (1σ; Fig. 5), an age that is only slightly younger than the youngest age peak at *c*. 290 Ma (Fig. 4).

Hf and Nd isotopes

Twenty-four zircons from the northeastern Eastern Andean Metamorphic Complex metasediments of the Argentine Bahía de la Lancha Formation (CA-01-06) and the Chilean Cochrane unit (CA-00-30) that were U–Pb dated were also analysed for their Hf-isotope compositions. Both samples display Carboniferous maximum depositional ages. To characterize the main sources, zircons with only one growth phase from the age peaks at 0.4–0.7 Ga and 0.9–1.4 Ga were preferentially selected. Except for two zircons with multiple growth phases (CA-01-06:45 and -06:63; not discussed further), all zircons have measured $^{176}Lu/^{177}Hf$ values of <0.002 and present-day $^{176}Hf/^{177}Hf$ values of

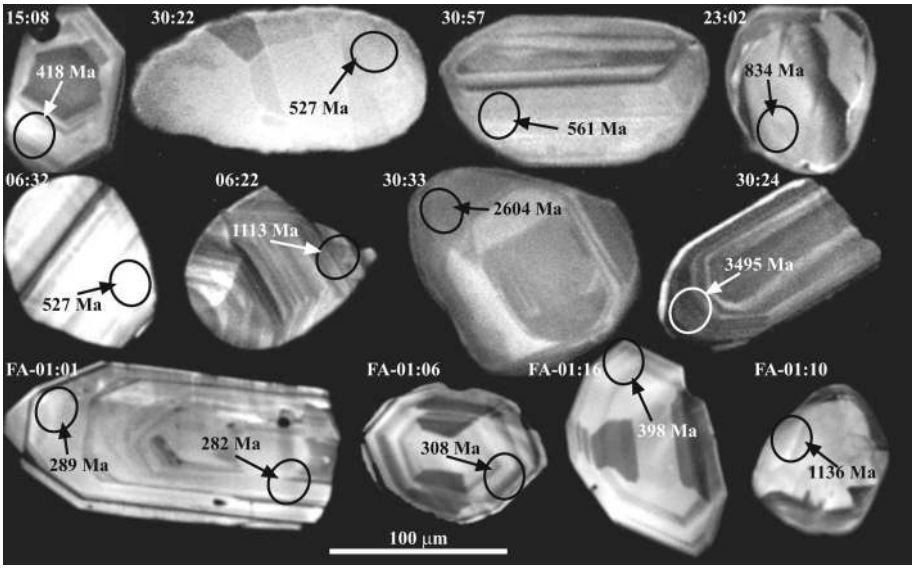

Fig. 3. Representative CL images of zircons that were used for U–Pb dating. Rounded zircons with metamorphic characteristics predominantly yielded ages >500 Ma, whereas euhedral and magmatically zoned zircons mainly gave ages <500 Ma. The Hf-isotope composition was determined for six of the zircons shown here (see Table 2).

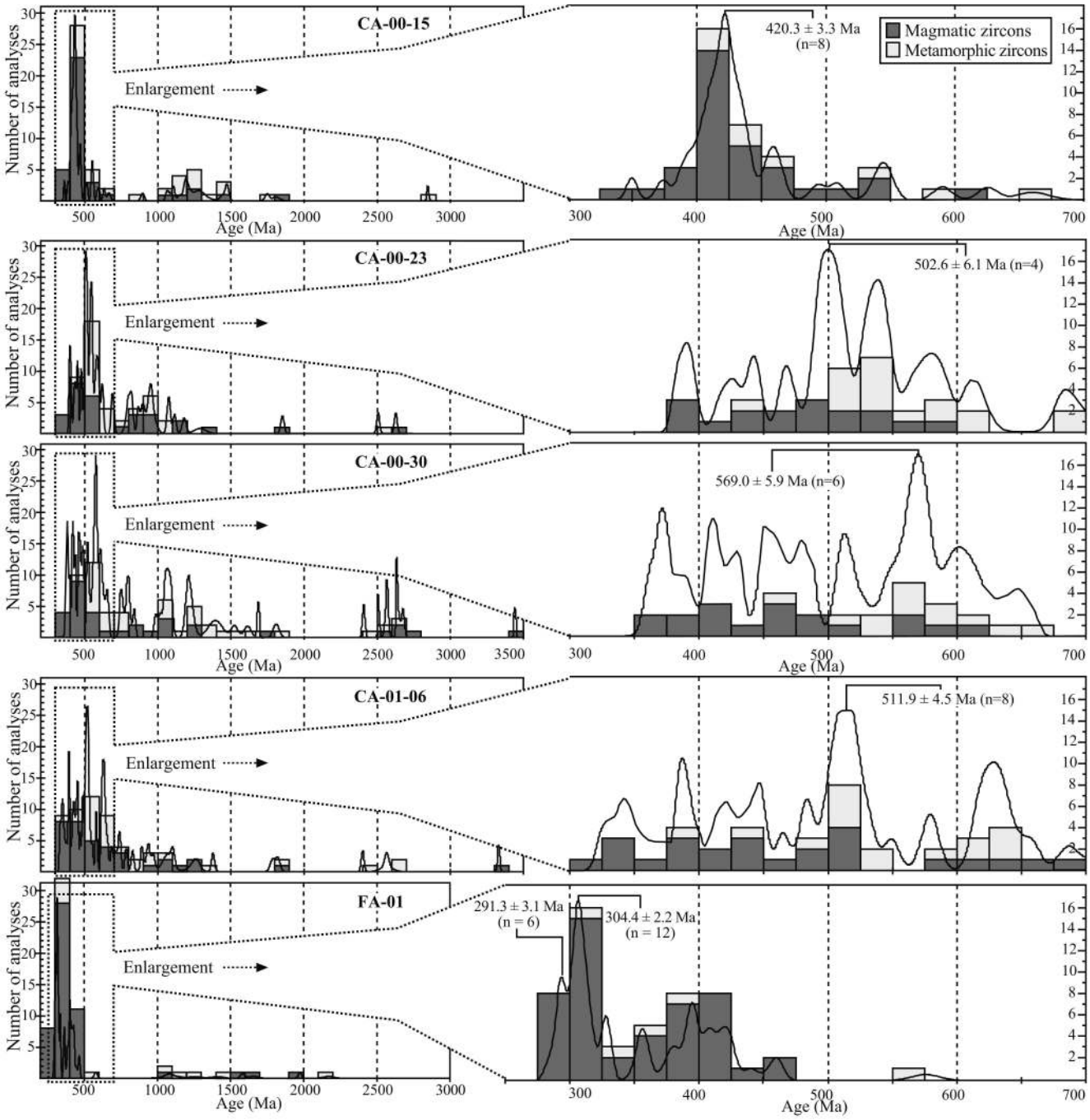

Fig. 4. U–Pb age distribution of analysed zircons with probability curves and weighted mean ages. The histogram bars represent time intervals of 100 Ma (left diagrams) and 25 Ma (enlarged diagrams to the right). Peak ages for CA-00-15 and FA-01 are calculated with magmatic zircons only (one metamorphic zircon was discarded from each of the *c*. 305 and 420 Ma peaks). Errors are given as 2σ. Background data are available online at http://www.geolsoc.org.uk/SUP18247. A hard copy can be obtained from the Society Library.

0.2805–0.2825, which correspond to present-day εHf values of −80 to −10 (Table 2).

The initial $^{176}Hf/^{177}Hf$ values expressed as $\varepsilon Hf_{(T)}$ indicate the Hf-isotope composition at the time of zircon crystallization and provide information about the evolution history of their crustal sources prior to crystallization of the zircons. In most cases, the analysed zircons with ages <0.7 Ga have lower $\varepsilon Hf_{(T)}$ values (−14 to +1) than those with ages of 0.9–1.65 Ga (-7 to +12; Fig. 6). The $\varepsilon Hf_{(T)}$ of two zircons with ages of 1.05 and 1.25 Ga overlap with depleted mantle values ($\varepsilon Hf_{(T)} = +12$). Thus, the protoliths of these two zircons can be regarded as juvenile. The negative $\varepsilon Hf_{(T)}$ of other zircons indicate crystallization from recycled old crustal material.

By extrapolating the crustal evolution paths for the zircons back in time, two-stage Lu–Hf model ages ($T_{DM}Hf^*$), which reflect the ingrowth of ^{176}Hf in the host-rock material prior to crystallization of a zircon at typical crustal Lu/Hf values ($^{176}Lu/^{177}Hf_{crust,today} = 0.0093$; average of granitoid data from

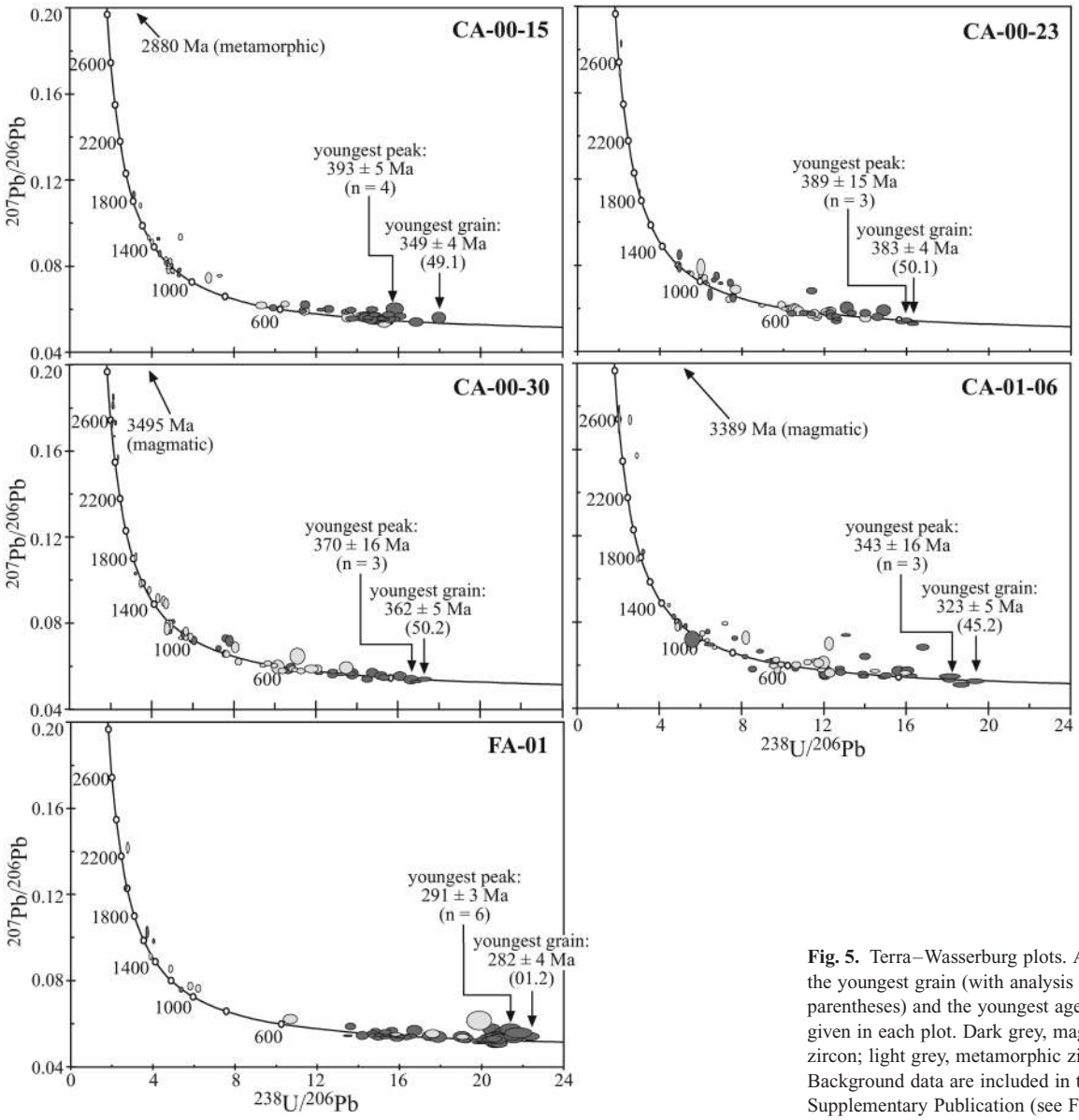

Fig. 5. Terra–Wasserburg plots. Ages for the youngest grain (with analysis number in parentheses) and the youngest age peak are given in each plot. Dark grey, magmatic zircon; light grey, metamorphic zircon. Background data are included in the Supplementary Publication (see Fig. 4).

Vervoort & Patchett 1996), can be calculated. For the <1.65 Ga old zircons most of the $T_{DM}Hf^*$ values fall in the ranges 1.2–1.4 Ga and 1.8–2.0 Ga (Table 2; Figs 6 and 7). The older zircons (2.4–3.5 Ga) display crustal residence ages of 2.9–3.8 Ga.

An advantage of using initial Hf-isotope compositions of zircons in provenance studies is the similarity between the Lu–Hf and Sm–Nd decay systems, in which the parent isotope is more compatible during crust formation than the corresponding daughter isotope. This leads to a relative enrichment of Hf and Nd in the crust, and to lower $^{176}Hf/^{177}Hf$ and $^{143}Nd/^{144}Nd$ than in the mantle. This effect leads to a strong coupling of εHf and εNd in most terrestrial rocks (e.g. Patchett 1983; Vervoort *et al*. 1999). Therefore, $T_{DM}Hf^*$ and two-stage Nd model ages ($T_{DM}Nd^*$) calculated for the same rock will correspond to each other if the isotopic evolution of the depleted mantle and typical crustal rocks are known. In Figure 7, Hf-isotope data are compared with previously reported Nd-isotope data (with references given in Table 3) for magmatic and metamorphic basement rocks in potential source areas in southern Gondwana. All Nd-isotope data were recalculated to $T_{DM}Nd^*$ with assumed first-stage crustal evolution from the value of the depleted mantle ($^{147}Sm/^{144}Nd_{DM,today} = 0.217$) and a present-day mean crustal $^{147}Sm/^{144}Nd$ of 0.11, which corresponds to $f = -0.44$. The $T_{DM}Nd^*$ values correspond to zircon $T_{DM}Hf^*$ calculated with $^{176}Lu/^{177}Hf$ values of 0.0093 and 0.0381 for average present-day crust and depleted mantle, respectively. The Lu/Hf and Sm/Nd values are average ratios inferred from a large set of crust and mantle samples (Goldstein *et al*. 1984; Albarède & Brouxel 1987; Vervoort & Patchett 1996; Vervoort & Blichert-Toft 1999; Vervoort *et al*. 2000).

Discussion

Tectonic evolution

Our U–Pb results are similar to age spectra of zircons from other Palaeozoic metasediments in south Patagonian Chile reported by Hervé *et al*. (2003). Likewise, the general age patterns change from broad age peaks in the samples with old maximum depositional ages to distinct narrow age peaks in samples with

Table 2. *Lutetium–hafnium isotope data*

	Zoning	$^{176}Lu/^{177}Hf$	$f^{Lu/Hf}$*	$^{176}Hf/^{177}Hf$ (today)	2σ ($\times 10^{-6}$)	ε_{Hf} (today)	Age† (Ma)	$^{176}Hf/^{177}Hf$ (initial)	ε_{Hf} (initial)	T_{DM} (Ma)	T_{DM}* (Ma)
Cochrane unit											
CA-00-30:01	Metamorphic	0.000364	−0.989	0.282083	21	−24.4	1398	0.282073	+6.3 ± 0.7	1598	1659
CA-00-30:02	Magmatic	0.000825	−0.975	0.282041	20	−25.9	1085	0.282024	−2.5 ± 0.7	1676	1848
CA-00-30:18	Magmatic	0.00100	−0.970	0.282482	23	−10.3	429	0.282474	−1.1 ± 0.8	1062	1243
CA-00-30:22	Metamorphic	0.0000228	−0.999	0.282223	14	−19.4	526	0.282222	−7.9 ± 0.5	1392	1668
CA-00-30:24	magmatic	0.00112	−0.966	0.280561	25	−78.2	3495	0.280486	−1.8 ± 0.9	3728	3794
CA-00-30:26	Metamorphic	0.000907	−0.973	0.282337	19	−15.4	1102	0.282318	+8.3 ± 0.7	1264	1311
CA-00-30:31	Metamorphic	0.000701	−0.979	0.281190	17	−55.9	2672	0.281154	+2.8 ± 0.6	2840	2890
CA-00-30:33	Magmatic	0.000376	−0.989	0.281082	21	−59.8	2604	0.281063	−2.0 ± 0.7	2961	3072
CA-00-30:36	Metamorphic	0.000373	−0.989	0.281207	23	−55.3	2439	0.281190	−1.3 ± 0.8	2793	2902
CA-00-30:37	Magmatic	0.00160	−0.952	0.282416	18	−12.6	484	0.282401	−2.5 ± 0.6	1174	1357
CA-00-30:42	Magmatic	0.000700	−0.979	0.281943	18	−29.3	1211	0.281927	−3.1 ± 0.6	1806	1983
CA-00-30:49	Metamorphic	0.000529	−0.984	0.281796	31	−34.5	1245	0.281784	−7.4 ± 1.1	2000	2227
CA-00-30:53	Metamorphic	0.000678	−0.980	0.281975	20	−28.2	1630	0.281954	+7.3 ± 0.7	1761	1800
CA-00-30:56	Magmatic	0.000987	−0.970	0.282334	14	−15.5	989	0.282315	+5.7 ± 0.5	1271	1352
CA-00-30:57	Metamorphic	0.0000910	−0.997	0.282032	15	−26.2	569	0.282032	−13.7 ± 0.5	1655	1999
CA-00-30:61	Magmatic	0.00179	−0.946	0.282249	19	−18.5	1221	0.282208	+7.1 ± 0.7	1421	1473
CA-00-30:64	Magmatic	0.000750	−0.977	0.282429	18	−12.1	578	0.282421	+0.3 ± 0.6	1129	1292
Bahía de la Lancha Formation											
CA-01-06:22	Magmatic	0.000508	−0.985	0.282059	21	−25.2	1113	0.282048	−1.0 ± 0.7	1637	1796
CA-01-06:25	Metamorphic	0.0000887	−0.997	0.282399	14	−13.2	629	0.282397	+0.6 ± 0.5	1152	1318
CA-01-06:32	Magmatic	0.000542	−0.984	0.282461	26	−11.0	1056	0.282450	+12.0 ± 0.9	1078	1085
CA-01-06:45‡	*Mix*	*0.00262*	*−0.921*	*0.282643*	*19*	*−4.5*	*323*	*0.282628*	*+2.0 ± 0.7*	*870*	*996*
CA-01-06:62	Magmatic	0.00104	−0.969	0.282232	20	−19.1	927	0.282214	+0.7 ± 0.7	1416	1554
CA-01-06:63‡	*Mix*	*0.000228*	*−0.993*	*0.281519*	*17*	*−44.3*	*711*	*0.281516*	*−28.8 ± 0.6*	*2362*	*2871*
CA-01-06:66	Magmatic	0.000827	−0.975	0.282335	19	−15.5	1252	0.282316	+11.6 ± 0.7	1264	1267

$T_{DM} = \ln[(^{176}Hf/^{177}Hf_{sample,today} - {}^{176}Hf/^{177}Hf_{DM,today})/(^{176}Lu/^{177}Hf_{sample,today} - {}^{176}Lu/^{177}Hf_{DM,today}) + 1]/\lambda$ and $T_{DM}* = \ln[(^{176}Lu/^{177}Hf_{sample,T} - {}^{176}Hf/^{177}Hf_{DM,T})/(^{176}Lu/^{177}Hf_{crust,T} - {}^{176}Lu/^{177}Hf_{DM,T}) + 1]/\lambda + T$, where T represents the zircon growth age. $^{176}Lu/^{177}Hf_{crust,T}$ was calculated assuming $^{176}Lu/^{177}Hf_{crust,today} = 0.0093$, average of granitoid data from Vervoort & Patchett (1996).

*Deviation of $^{176}Lu/^{177}Hf$ from CHUR: $f^{Lu/Hf} = (^{176}Lu/^{177}Hf_{sample,today}/^{176}Lu/^{177}Hf_{CHUR,today}) - 1$.

†U–Pb zircon ages

‡Grain with several growth phases; corresponding values were not used further.

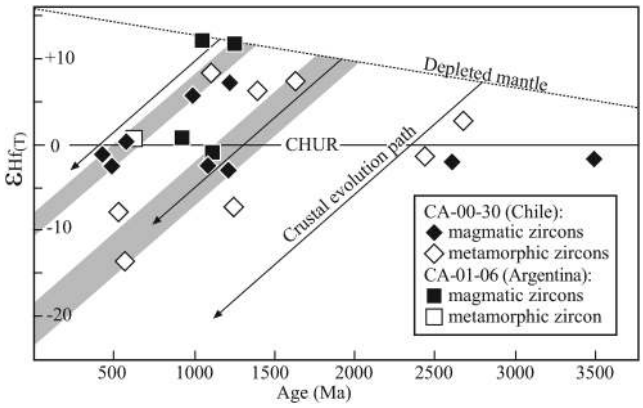

Fig. 6. U–Pb ages and $\varepsilon Hf_{(T)}$ for single detrital zircon grains. Arrows indicate typical crustal evolution paths, assuming $^{176}Lu/^{177}Hf_{crust,today} = 0.0093$ (average of granitoid data from Vervoort & Patchett 1996; see also Scherer *et al*. 2001). The 2σ errors of $\varepsilon Hf_{(T)}$ are smaller than the symbols (see Table 2). Shaded areas represent crustal evolution paths of zircons that might originate from common domains. Evolution of the depleted mantle, $\varepsilon Hf_{(T)}$ and $T_{DM}Hf^*$ were calculated with $\lambda(^{176}Lu) = 1.865 \times 10^{-11}$ (Scherer *et al*. 2001), $^{176}Lu/^{177}Hf_{CHUR,today} = 0.0332$, $^{176}Hf/^{177}Hf_{CHUR,today} = 0.282772$ (Blichert-Toft & Albarède 1997), $^{176}Lu/^{177}Hf_{DM,today} = 0.0381$, and $^{176}Lu/^{177}Hf_{DM,today} = 0.283224$ (Vervoort *et al*. 2000).

young maximum depositional ages. The sampling of lithologically similar metasediments (turbiditic metagreywackes) makes it likely that the U–Pb age spectra presented here and by Hervé *et al*. (2003) mirror changes in tectonic configuration along the Palaeozoic south Patagonian proto-Pacific margin of Gondwana (see DeGraaff-Surpless *et al*. 2003). An active tectonic regime often implies rapid new exposure of potential source rocks. Therefore, sediments deposited in active margin basins are less severely affected by recycling than passive margin sediments, and they will have a larger detrital supply from local sources (Potter 1978; Veizer & Jansen 1985; McLennan & Taylor 1991).

We interpret the differences in zircon populations to mark the change from a passive margin regime to the onset of eastward subduction and the development of a magmatic arc in Late Carboniferous time in southern Patagonia (see also Hervé *et al*. 2003). This is consistent with an earlier interpretation based on whole-rock element and Nd-isotope data (Augustsson & Bahlburg 2003), and is in accordance with onset of subduction at the latest at *c*. 300 Ma in northern Patagonia (see Willner *et al*. 2004*a*) and Late Carboniferous onset of subduction beyond Patagonia further along the margin in central and northern Chile (Bahlburg & Hervé 1997; Willner *et al*. 2005).

The youngest zircons and the U–Pb age spectra point to (Late Devonian to) Carboniferous deposition for the passive-margin northeastern Eastern Andean Metamorphic Complex sediments (see Fig. 2). Deposition of the southwestern Eastern Andean Metamorphic Complex metasediment probably took place in Early Permian time, slightly after crystallization of the youngest dated zircon.

Sources of Early to Late Carboniferous metasediments

Potential source regions for detritus of the Patagonian passive margin sediments include present-day northern Chile and Argentina, Brazil, Uruguay, southern Africa, the Falkland Islands and Antarctica. Hervé *et al*. (2003) considered most of these areas as possible source areas for late Palaeozoic Chilean metasediments

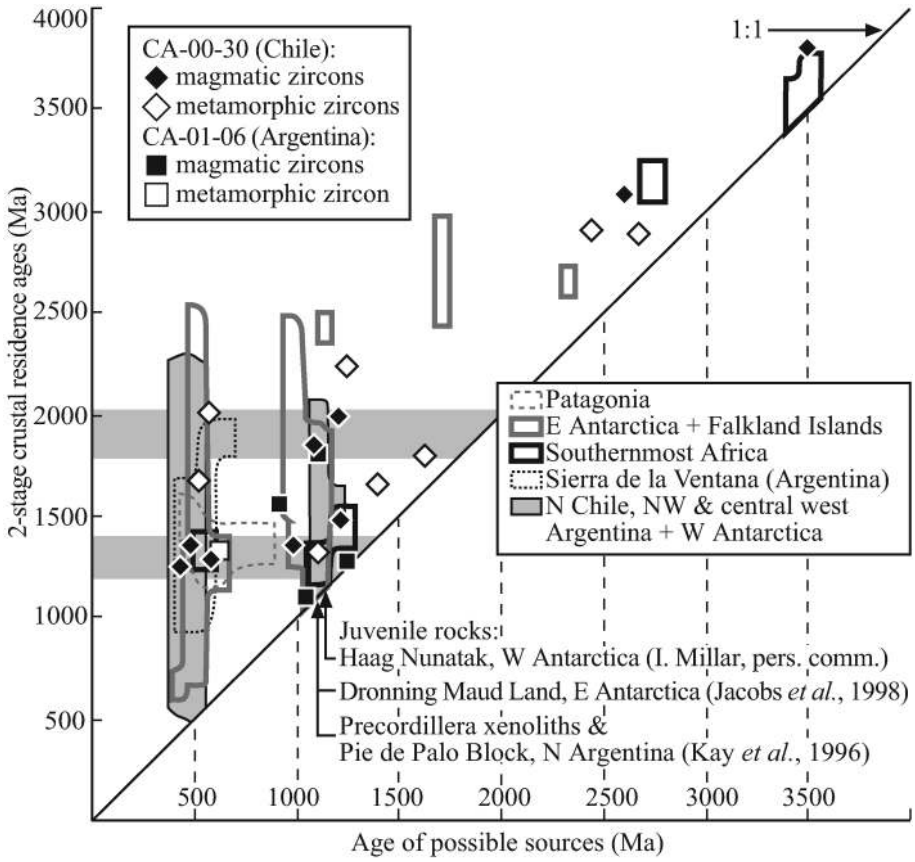

Fig. 7. Recalculated whole-rock two-stage model ages plotted against absolute ages of rocks (≥400 Ma) in various provinces of southern Gondwana. Hf model ages of Patagonian passive margin sediments (CA-00-30 and CA-01-06) with corresponding U–Pb zircon ages are plotted for comparison. Horizontal grey areas represent model age intervals of zircons that might originate from common domains.

Table 3. *References to Nd and Hf isotope data* for possible source areas of the Patagonian sediments*

Area	Ref.	Area	Ref.	Area	Ref.
Argentine Patagonia (n = 5)		*West Antarctica (n = 4)*		*Northern Chile, northern and central Argentina (n = 177)*	
Colohuincul Complex	1	Haag Nunatak	8†‡, 9	Chilean Precordillera	17
Deseado Massif	2	Target Hill	10	Cordillera de la Costa, northern Chile	17
				Cuyania terrane, NW Argentina	18
Falkland Islands and Plateau (n = 11)		*East Antarctica (n = 116)*		Las Matras Block, central Argentina	19
Cape Meredith Complex	3, 4	Coats Land	9	Las Termas Belt, NW Argentina	20
Maurice Ewing Bank	4	Dronning Maud Land	4, 11	Pie de Palo Block, northern Argentina	21†
		Mawson Coast	12	Precordillera xenoliths, northern Argentina	21†
Southernmost Africa (n = 19)		Prince Charles Mts	13	Puna, NW Argentina and northern Chile	17, 22
Barberton Greenstone Belt, South Africa	5	Shackleton Range	14	San Rafael Block, central Argentina	23
Cape Granite suite, South Africa	6	Transantarctic Mts	15	Sierra de Medina, NW Argentina	17
Mkhondo suite, Swaziland	7			Sierras Pampeanas, northern Argentina	17, 24
Natal Metamorphic Province, South Africa	4	*Sierra de la Ventana, Argentina (n = 9)*	16		

Nd isotope data were recalculated to $T_{DM}{}^{*} = \ln[(^{143}Nd/^{144}Nd_{sample,Ts} - {}^{143}Nd/^{144}Nd_{DM,Ts})/(^{147}Sm/^{144}Nd_{crust,Ts} - {}^{147}Sm/^{144}Nd_{DM,Ts}) + 1]/\lambda + T_s$, where T_s is the rock age, $\lambda = 6.54 \times 10^{-12}a^{-1}$, $^{143}Nd/^{144}Nd_{DM,today} = 0.51315$ and $^{147}Sm/^{144}Nd_{DM,today} = 0.217$. $^{147}Sm/^{144}Nd_{crust,Ts}$ was calculated assuming $^{147}Sm/^{144}Nd_{crust,today} = 0.11$. References: 1, Dalla Salda *et al*. (1991); 2, Pankhurst *et al*. (2003); 3, Thistlewood *et al*. (1997), Thomas *et al*. (1998); 4, Wareham *et al*. (1998); 5, Kröner *et al*. (1996); 6, da Silva *et al*. (2000); 7, Condie *et al*. (1996); 8, I. Millar (pers. comm.); 9, Storey *et al*. (1994); 10, Milne & Millar (1989); 11, Arndt *et al*. (1991), Jacobs *et al*. (1998), Paulsson & Austrheim (2003), Ravikant *et al*. (2004); 12, Young *et al*. (1997); 13, Zhao *et al*. (1997); 14, Brommer *et al*. (1999); 15, Wareham *et al*. (2001); 16, Rapela *et al*. (2003); 17, Lucassen *et al*. (2000); 18, Porcher *et al*. (2004); 19, Sato *et al*. (2000); 20, Höckenreiner *et al*. (2003); 21, Kay *et al*. (1996); 22, Bock *et al*. (2000), Poma *et al*. (2004); 23, Cingolani *et al*. (2003); 24, Pankhurst *et al*. (1998), Rapela *et al*. (1998), Steenken *et al*. (2004).

The literature data form the basis for T_{DM}Hf and T_{DM}Nd* of rocks from possible source areas shown in Figure 7.

†Isotope values used as published.

‡Hf-isotope data. All other data are Nd-isotope data.

of the northeastern Eastern Andean Metamorphic Complex. However, the scarcity of Transamazonian ages (c. 2 Ga) in the U–Pb age spectra (Hervé *et al*. 2003; this study) precludes the Brazilian Amazonian and São Francisco cratons, the Rio de La Plata Craton in Uruguay and northeastern Argentina, and the South African Bushveld Complex as possible important source regions.

The youngest (<0.5 Ga) zircon population might predominantly originate from Patagonia itself. This is indicated by the *c*. 420 Ma zircon age peaks of largely magmatic zircons and the abundance of 450–500 Ma old zircons (Fig. 4), which overlap with granitic magmatism in eastern Patagonia (Pankhurst *et al*. 2003). One of the analysed zircons (T *c*. 480 Ma) has a T_{DM}Hf* of *c*. 1360 Ma, similar to the east Patagonian granites (Fig. 7; T_{DM}Nd* *c*. 1.5 Ga; Pankhurst *et al*. 2003). A local Patagonian origin is supported by the zircon morphology. Of the 78 zircons with ages <0.5 Ga, 83% are weakly abraded, whereas 80% of the older grains are subrounded to rounded.

Most of the U–Pb dated zircons have crystallization ages between 0.5 and 0.6 Ga (Fig. 4), and most potential source areas beyond Patagonia in southern Gondwana are dominated by *c*. 0.5 and 1.0–1.2 Ga magmatic and metamorphic rocks with overlapping T_{DM}Nd* (≤2.5 Ga; Fig. 7). Many of the Patagonian zircons in both age ranges display T_{DM}Hf* of 1.2–1.4 and 1.8–2.0 Ga. Provided that the Hf-isotope composition of the source material evolved following inferred typical crustal evolution paths, the zircons with similar model ages might all originate from similar crustal domains despite their large range in $\varepsilon Hf_{(T)}$. Therefore, the dominant source areas need to account for the presence of both 0.5–0.6 Ga and 1.0–1.2 Ga old zircons with model ages of 1.2–1.4 and 1.8–2.0 Ga. Furthermore, they have to explain the presence of both juvenile and recycled 1.0–1.3 Ga zircons ($\varepsilon Hf_{(T)} = -7$ to +12).

East Antarctica as well as northern Chile and northwestern and central western Argentina along the margin of Gondwana are possible source areas with magmatic and metamorphic felsic rocks of 0.5–0.6 Ga and *c*. 1.0–1.2 Ga, and with T_{DM}Nd* of both *c*. 1.2–1.4 and *c*. 1.8–2.0 Ga (e.g. Kay *et al*. 1996; Jacobs *et al*. 1998; Lucassen *et al*. 2000; Paulsson & Austrheim 2003). This includes juvenile *c*. 1.1 Ga gneisses from Dronning Maud Land (Jacobs *et al*. 1998) and central western Argentina (Kay *et al*. 1996) as potential source rock candidates for the juvenile *c*. 1060 Ma zircon (T_{DM}Hf* = 1085 Ma). Likewise, West Antarctica and the Falkland Plateau have both juvenile gneiss (Hf model age at Haag Nunatak; I. Millar, pers. comm.) and recycled *c*. 1.1 Ga old felsic rocks (T_{DM}Nd* = 1.2–1.6 Ga, Cape Meredith Complex and Maurice Ewing Bank; Thistlewood *et al*. 1997; Wareham *et al*. 1998). However, West Antarctic and Falkland Plateau sources cannot explain the dominance of 0.5–0.6 Ga zircons.

The Sierra de la Ventana north of Patagonia and the Cape Granite Suite in South Africa could be further sources for 0.5–0.6 Ga old zircons. Here, granites and rhyolites occur, of which the T_{DM}Nd* values (1.1–1.9 Ga; da Silva *et al*. 2000; Rapela *et al*. 2003) overlap with those of the detrital zircons (1.3–2.0 Ga; see Fig. 7). Furthermore, gneisses of the Natal Metamorphic province in South Africa with 1.2 Ga protolith ages and T_{DM}Nd* of *c*. 1.4 Ga (Wareham *et al*. 1998) could explain the presence of a *c*. 1250 Ma juvenile (T_{DM}Hf* = 1267 Ma) zircon analysed for its Hf-isotope composition. Southernmost Africa is also a probable source for the 2.4–3.5 Ga zircon population with T_{DM}Hf* of 2.9–3.8 Ga (Fig. 7; Kaapvaal Craton rock ages are *c*. 2.7 and

3.5 Ga with $T_{DM}Nd^* = 3.1–3.8$ Ga; Condie *et al*. 1996; Kröner *et al*. 1996).

The zircons in the 1.4–1.7 Ga age range ($T_{DM}Hf^*$ *c*. 1660 and 1800 Ma) might have arrived from parts of the present South American continent north and NW of the Sierra de la Ventana, such as the Rio Negro–Juruena orogenic belt of the Amazonian Craton (magmatic and metamorphic rock ages 1.4–1.8 Ga, $T_{DM}Nd^* = 1.6–2.0$ Ga; Geraldes *et al*. 2001). However, because of the low content of zircons in the age ranges 1.4–1.7 Ga in the metasediments (Fig. 4), the belt can have been of only minor importance as a source of the detrital zircon population of the metasediments. Thus, the most probable dominant source areas for the Carboniferous metasediments were the interior of Gondwana (Patagonia, the Sierra de la Ventana, southernmost Africa and East Antarctica) and the proto-Pacific coast further north of Patagonia (see Fig. 8).

The proposed derivation of zircons with ages >500 Ma from the interior of Gondwana can be explained by sediment recycling and the presence of erosional barriers that cut through southern Africa and southern South America north of Patagonia (Fig. 8). Furthermore, transport of large volumes of sediment from the interior of Gondwana to Patagonia implies that Patagonia had an autochthonous position relative to Gondwana during times of transport and deposition of the Patagonian sediments. Considering the suggested sediment transportation paths, a collision of Patagonia with Gondwana in Permian to Triassic time as previously proposed (see Ramos 1984) is unlikely.

Sources of Early Permian metasediments

The dominance of <0.5 Ga old zircons in the Early Permian metasediment (FA-01, southwestern Eastern Andean Metamorphic Complex) suggests that the detrital supply from the interior of Gondwana had ceased by the Early Permian. The zircons representing the two youngest age peaks at *c*. 290 and 305 Ma in the age spectrum might originate from igneous rocks of similar ages in present-day Andean Patagonia (*c*. 290, 300 and 305 Ma; Martin *et al*. 1999; R. de la Cruz, pers. comm.) and on the Falkland Islands (*c*. 305 Ma; Thistlewood *et al*. 1997), whereas the zircons making up the peaks at *c*. 325 Ma, 390 Ma and 1.0–1.2 Ga overlap with ages of granites and gneisses in West Antarctica (Millar & Pankhurst 1987; Millar *et al*. 2001). Present-day extra-Andean Patagonia might be the source of 400–500 Ma old zircons (magmatism at *c*. 425 Ma and 470 Ma; see Pankhurst *et al*. 2003).

Conclusions

The U–Pb ages of the zircons in the Patagonian metasedimentary rocks give new maximum estimates for the timing of deposition of the Cochrane unit and Bahía de la Lancha Formation of the northeastern Eastern Andean Metamorphic Complex, as well as for the southwestern Eastern Andean Metamorphic Complex. Maximum depositional ages are *c*. 385–350 Ma, *c*. 330 Ma and *c*. 290 Ma, respectively. The U–Pb age data support a model in which subduction along the south Patagonian margin of Gondwana commenced in Late Carboniferous time, or at the latest in Early Permian time. Combined U–Pb ages and initial Hf-isotope compositions of single zircons reveal source areas for the Carboniferous passive margin sediments in the interior of Gondwana (Patagonia, the Sierra de la Ventana, East Antarctica and southern Africa), as well as coast-parallel sediment transport from northern Chile and northwestern Argentina (Fig. 8). This is consistent with an autochthonous origin of Patagonia relative to Gondwana. In contrast to the Carboniferous sediments, the Permian sediment was probably largely supplied

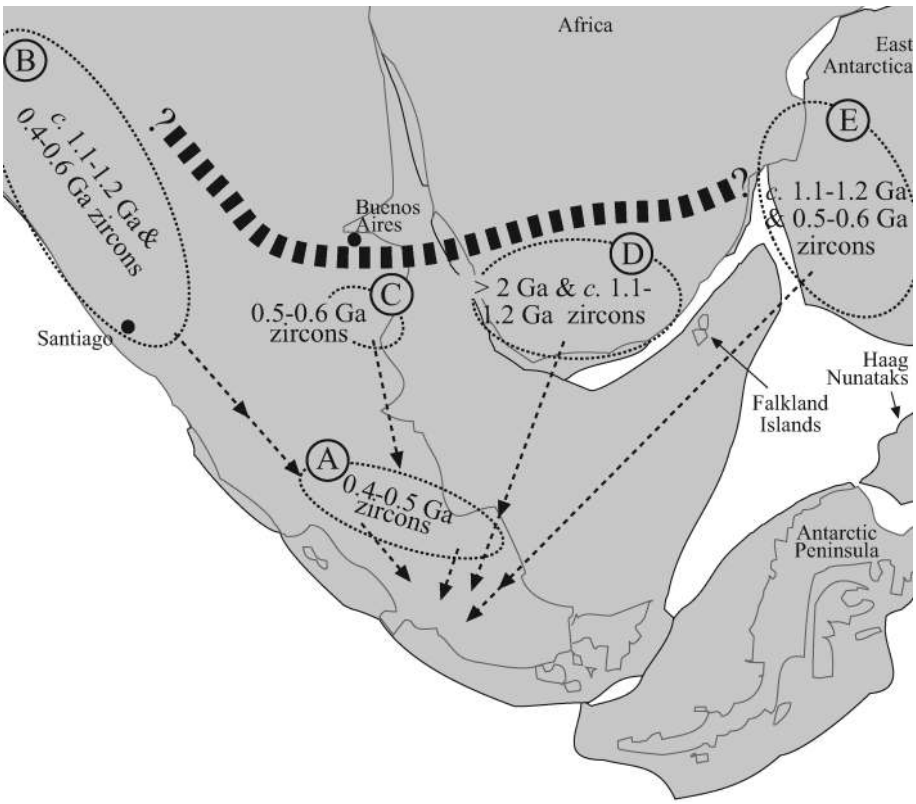

Fig. 8. Proposed source areas of the Patagonian passive margin sediments (see also Hervé *et al*. 2003, fig. 9) shown in a Gondwana reconstruction after Lawver & Scotese (1987). The position of the Falkland Islands is from Taylor & Shaw (1989). A, Extra-Andean Patagonia; B, northern Chile and northwestern Argentina; C, the Sierra de la Ventana; D, southernmost Africa; E, East Antarctica. Thick dotted line shows approximate position of proposed Carboniferous erosion barrier(s).

from local Patagonian, and West Antarctic sources. The central Gondwana sources were possibly cut off by the developing collision along the southwestern South American margin of Gondwana.

This work was supported by the Deutsche Forschungsgemeinschaft (DFG; grant Ba 1011/17-3). It is a contribution to IGCP project 471 'Evolution of western Gondwana during the late Palaeozoic: tectonosedimentary record, palaeoclimates and biological changes'. R. Pankhurst is thanked for valuable comments on an earlier version of the paper. U. Söderlund and I. Millar are gratefully acknowledged for comments that considerably improved the paper.

References

Albarède, F. & Brouxel, M. 1987. The Sm/Nd secular evolution of the continental crust and the depleted mantle. *Earth and Planetary Science Letters*, **82**, 25–35.

Amelin, Y., Lee, D.-C., Halliday, A.N. & Pidgeon, R.T. 1999. Nature of the Earth's earliest crust from hafnium isotopes in single detrital grains. *Nature*, **399**, 252–255.

Amelin, Y., Lee, D.-C. & Halliday, A.N. 2000. Early–middle Archaean crustal evolution deduced from Lu–Hf and U–Pb isotopic studies of single zircon grains. *Geochimica et Cosmochimica Acta*, **64**, 4205–4225.

Arndt, N.T., Todt, W., Chauvel, C., Tapfer, M. & Weber, K. 1991. U–Pb zircon age and Nd isotopic composition of granitoids, charnockites and supracrustal rocks from Heimfrontfjella, Antarctica. *Geologische Rundschau*, **80**, 759–777.

Augustsson, C. & Bahlburg, H. 2003. Active or passive margin? Geochemical and Nd isotope constraints of metasediments in the backstop of a pre-Andean accretionary wedge in southernmost Chile (46°30′–48°30′S). *In:* McCann, T. & Saintot, A. (eds) *Tracing Tectonic Deformation using the Sedimentary Record*. Geological Society, London, Special Publications, **208**, 253–268.

Augustsson, C., Bahlburg, H. & Münker, C. 2004. Conventional versus novel provenance techniques—example from the Palaeozoic Patagonia (Chile and Argentina). *Schriftreihe der Deutschen Geologischen Gesellschaft*, **33**, 18.

Bahlburg, H. & Hervé, F. 1997. Geodynamic evolution and tectonostratigraphic terranes of northwestern Argentina and northern Chile. *Geological Society of America Bulletin*, **109**, 869–884.

Blichert-Toft, J. 2001. On the Lu–Hf isotope geochemistry of silicate rocks. *Geostandards Newsletter*, **25**, 41–56.

Blichert-Toft, J. & Albarède, F. 1997. The Lu–Hf isotope geochemistry of chondrites and the evolution of the mantle–crust system. *Earth and Planetary Science Letters*, **148**, 243–258.

Bock, B., Bahlburg, H., Wörner, G. & Zimmermann, U. 2000. Tracing crustal evolution in the southern central Andes from Late Precambrian to Permian with geochemical and Nd and Pb isotope data. *Journal of Geology*, **108**, 515–535.

Bodet, F. & Schärer, U. 2000. Evolution of the SE-Asian continent from U–Pb and Hf isotopes in single grains of zircon and baddeleyite from large rivers. *Geochimica et Cosmochimica Acta*, **64**, 2067–2091.

Brommer, A., Millar, I.L. & Zeh, A. 1999. Geochronology, structural geology and petrology of the northwestern La Grange Nunataks, Shackleton Range, Antarctica. *Terra Antartica*, **6**, 269–278.

Chernicoff, C.J. & Zappettini, E.O. 2004. Geophysical evidence for terrane boundaries in south–central Argentina. *Gondwana Research*, **7**, 1105–1116.

Cingolani, C. A., Basei, M. A. S., Llambías, E. J., Varela, R., Chemale, F., Jr, Siga, O., Jr & Abre, P. 2003. The Rodeo Bordalesa Tonalite, San Rafael Block (Argentina): geochemical and isotopic age constraints. *In: 10° Congreso Geológico Chileno, Concepción, Actas* (CD-ROM).

Claoué-Long, J.C., Compston, W., Roberts, J. & Fanning, C.M. 1995. Two Carboniferous ages: a comparison of SHRIMP zircon dating with conventional zircon ages and $^{40}Ar/^{39}Ar$ analysis. *In:* Berggren, W.A., Kent, D.V., Aubry, M.-P. & Hardenbol, J. (eds) *Geochronology, Time Scales and Global Stratigraphic Correlation*. Society of Economic Paleontologists and Mineralogists, Special Publications, **54**, 3–21.

Condie, K.C., Kröner, A. & Milisenda, C.C. 1996. Geochemistry and geochronology of the Mkhondo suite, Swaziland: evidence for passive-margin deposition and granulite facies metamorphism in the Late Archean of Southern Africa. *Journal of African Earth Sciences*, **21**, 483–506.

Cumming, G.L. & Richards, J.R. 1975. Ore lead isotope ratios in a continuously changing earth. *Earth and Planetary Science Letters*, **28**, 155–171.

Dalla Salda, L., Cingolani, C.A. & Varela, R. 1991. El basamento pre-andino igneo metamórfico de San Martín de los Andes, Neuquén. *Asociación Geológica Argentina Revista*, **46**, 223–234.

Dalziel, I.W.D. & Grunow, A.M. 1992. Late Gondwanide tectonic rotations within Gondwanaland. *Tectonics*, **11**, 603–606.

da Silva, L.C., Gresse, P.G., Scheepers, R., McNaughton, N.J., Hartmann, L.A. & Fletcher, I. 2000. U–Pb SHRIMP and Sm–Nd age constraints on the timing and sources of the Pan-African Cape Granite Suite, South Africa. *Journal of African Earth Sciences*, **30**, 795–815.

DeGraaff-Surpless, K., Mahoney, J.B., Wooden, J.L. & McWilliams, M.O. 2003. Lithofacies control in detrital zircon provenance studies: insights from the Cretaceous Methow basin, southern Canadian Cordillera. *Geological Society of America Bulletin*, **115**, 899–915.

Douglass, R.C. & Nestell, M.K. 1976. *Late Paleozoic Foraminifera from Southern Chile*. US Geological Survey, Professional Papers, **858**.

Escobar, F. (ed.) 1980. *Mapa Geológico de Chile, 1:1 000 000*. Servicio Nacional de Geología y Minería.

Fang, Z., Boucot, A., Covacevich, V. & Hervé, F. 1998. Discovery of Late Triassic fossils in the Chonos Metamorphic Complex, Southern Chile. *Revista Geológica de Chile*, **25**, 165–174.

Forsythe, R. 1982. The late Palaeozoic to early Mesozoic evolution of southern South America: a plate tectonic interpretation. *Journal of the Geological Society, London*, **139**, 671–682.

Fortey, R., Pankhurst, R.J. & Hervé, F. 1992. Devonian Trilobites at Buill, Chiloé (42°S). *Revista Geológica de Chile*, **19**, 133–143.

Geraldes, M.C., Van Schmus, W.R., Condie, K.C., Bell, S., Teixeira, W. & Babinski, M. 2001. Proterozoic geologic evolution of the SW part of the Amazonian Craton in Mato Grosso state, Brazil. *Precambrian Research*, **111**, 91–128.

Giacosa, R.E. 1999. El basamento pre-silúrico del extremo este del Macizo Nordpatagónico y del Macizo del Deseado. *In:* Caminos, R. (ed.) *Geología Argentina*. Instituto de Geología y Recursos Minerales, Anales, **29**, 118–123.

Goldstein, S.L., O'Nions, R.K. & Hamilton, P.J. 1984. A Sm–Nd study of atmospheric dusts and particulates from major river systems. *Earth and Planetary Science Letters*, **70**, 221–236.

Hervé, F., Fanning, C.M. & Pankhurst, R.J. 2003. Detrital zircon age patterns and provenance of the metamorphic complexes of southern Chile. *Journal of South American Earth Sciences*, **16**, 107–123.

Höckenreiner, M., Söllner, F. & Miller, H. 2003. Dating the TIPA shear zone: an Early Devonian terrane boundary between the Famatinian and Pampean systems (NW Argentina). *Journal of South American Earth Sciences*, **16**, 45–66.

Jacobs, J., Fanning, C.M., Henjes-Kunst, F., Olesch, M. & Paech, H.-J. 1998. Contribution of the Mozambique Belt into East Antarctica: Grenville-age metamorphism and polyphase Pan-African high-grade events in Central Dronning Maud Land. *Journal of Geology*, **106**, 385–406.

Jaffey, A.H., Flynn, K.F., Glendenin, L.E., Bentley, W.C. & Essling, A.M. 1971. Precision measurement of half-lives and specific activities of ^{235}U and ^{238}U. *Physical Review C*, **4**, 1889–1906.

Kay, S.M., Orrell, S. & Abbruzzi, J. 1996. Zircon and whole rock Nd–Pb isotopic evidence for a Grenville age and a Laurentian origin for the basement of the Precordillera in Argentina. *Journal of Geology*, **104**, 637–648.

Knudsen, T.-L., Griffin, W.L., Hartz, E.H., Andresen, A. & Jackson, S.E. 2001. *In situ* hafnium and lead isotope analyses of detrital zircons from the Devonian sedimentary basin of NE Greenland: a record of repeated crustal reworking. *Contributions to Mineralogy and Petrology*, **141**, 83–94.

Kröner, A., Hegner, E., Wendt, J.I. & Byerly, G.R. 1996. The oldest part of the Barberton granitoid–greenstone terrain, South Africa: evidence for crust formation between 3.5 and 3.7 Ga. *Precambrian Research*, **78**, 105–124.

Lawver, L.A. & Scotese, C.R. 1987. A revised reconstruction of Gondwanaland. *In:* McKenzie, G.D. (ed.) *Gondwana Six: Structure, Tectonics and Geophysics*. Geophysical Monographs, American Geophysical Union, **40**, 17–23.

Ling, H.Y. & Forsythe, R.D. 1987. Late Paleozoic pseudoalbaillellid radiolarians from southernmost Chile and their geological significance. *In:* McKenzie, D.G. (ed.) *Gondwana Six: Structure, Tectonics and Geophysics*. Geophysical Monographs, American Geophysical Union, **40**, 253–260.

Ling, H.Y., Forsythe, R.D. & Douglass, R.C. 1985. Late Paleozoic microfaunas from southernmost Chile and their relation to Gondwanaland forearc development. *Geology*, **13**, 357–360.

Lucassen, F., Becchio, R., Wilke, H.G., Franz, G., Thirlwall, M.F., Viramonte, J. & Wemmer, K.P. 2000. Proterozoic–Paleozoic development of the basement of the Central Andes (18–26°S)—a mobile belt of the South American craton. *Journal of South American Earth Sciences*, **13**, 697–715.

Ludwig, K.R. 2001a. *SQUID 1.02, a User's Manual*. Berkeley Geochronology Centre Special Publications, **2**.

Ludwig, K.R. 2001b. *User's Manual for Isoplot/Ex rev. 2.49, a Geochronological Toolkit for Microsoft Excel*. Berkeley Geochronology Centre Special Publications, **1a**.

Martin, M.W., Kato, T.T., Rodriguez, C., Godoy, E., Duhart, P., McDonough, M. & Campos, A. 1999. Evolution of the late Paleozoic accretionary

complex and overlying forearc–magmatic arc, south central Chile (38°–41°S): constraints for the tectonic setting along the southwestern margin of Gondwana. *Tectonics*, **18**, 582–356.

McLennan, S.M. & Taylor, S.R. 1991. Sedimentary rocks and crustal evolution: tectonic setting and secular trends. *Journal of Geology*, **99**, 1–21.

Millar, I.L. & Pankhurst, R.J. 1987. Rb–Sr geochronology of the region between the Antarctic Peninsula and the Transantarctic Mountains: Haag Nunataks and Mesozoic granitoids. *In:* McKenzie, G.D. (ed.) *Gondwana Six: Structure, Tectonics and Geophysics*. Geophysical Monographs, American Geophysical Union, **40**, 151–160.

Millar, I.L., Willan, R.C.R., Wareham, C.D. & Boyce, A.J. 2001. The role of crustal and mantle sources in the genesis of granitoids of the Antarctic Peninsula and adjacent crustal blocks. *Journal of the Geological Society, London*, **158**, 855–867.

Milne, A.J. & Millar, I.L. 1989. The significance of mid-Palaeozoic basement in Graham Land, Antarctic Peninsula. *Journal of the Geological Society, London*, **146**, 207–210.

Münker, C., Weyer, S., Scherer, E. & Mezger, K. 2001. Separation of high field strength elements (Nb, Ta, Zr, Hf) and Lu from rock samples for MC-ICPMS measurements. *Geochemistry, Geophysics, Geosystems*, **2**, doi:10.1029/2001GC000183.

Nebel-Jacobsen, Y., Scherer, E.E., Münker, C. & Mezger, K. 2005. Separation of U, Pb, Lu, and Hf from single zircons for combined U–Pb dating and Hf isotope measurements by TIMS and ICPMS. *Chemical Geology*, **220**, 105–120.

Nullo, F.E., Proserpio, C. & Ramos, V.A. 1978. Estratigrafía y tectónica de la vertiente este del hielo continental patagónico, Argentina–Chile. *In: VII Congreso Geológico Argentino, Neuquén, Actas*, **1**, 455–470.

Paces, J.B. & Miller, J.D. Jr 1993. Precise U–Pb ages of Duluth Complex and related mafic intrusions, northeastern Minnesota: geochronological insights to physical, petrogenetic, paleomagnetic, and tectonomagmatic processes associated with the 1.1 Ga midcontinent rift system. *Journal of Geophysical Research, 98B*, 13997–14013.

Pankhurst, R.J., Rapela, C.W., Saavedra, J., Baldo, E., Dahlquist, J., Pascua, I. & Fanning, C.M. 1998. The Famatinian magmatic arc in the central Sierras Pampeanas: an Early to Mid-Ordovician continental arc on the Gondwana margin. *In:* Pankhurst, R.J. & Rapela, C.W. (eds) *The Proto-Andean Margin of Gondwana*. Geological Society, London, Special Publications, **142**, 343–367.

Pankhurst, R.J., Rapela, C.W., Loske, W.P., Márquez, M. & Fanning, C.M. 2003. Chronological study of pre-Permian basement rocks of Southern Patagonia. *Journal of South American Earth Sciences*, **16**, 27–44.

Patchett, P.J. 1983. Importance of the Lu–Hf isotopic system in studies of planetary chronology and chemical evolution. *Geochimica et Cosmochimica Acta*, **47**, 81–91.

Paulsson, O. & Austrheim, H. 2003. A geochronological and geochemical study of rocks from Gjelsvikfjella, Dronning Maud Land, Antarctica—implications for Mesoproterozoic correlations and assembly of Gondwana. *Precambrian Research*, **125**, 113–138.

Poma, S., Quenardelle, S., Litvak, V., Maisonnave, E.B. & Koukharsky, M. 2004. The Sierra de Macon, plutonic expression of the Ordovician magmatic arc, Salta Province Argentina. *Journal of South American Earth Sciences*, **16**, 587–597.

Porcher, C.C., Fernandes, L.A.D., Vujovich, G.I. & Chernicoff, C.J. 2004. Thermobarymetry, Sm/Nd ages and geophysical evidence for the location of the suture zone between Cuyania and the western proto-Andean Margin of Gondwana. *Gondwana Research*, **7**, 1057–1076.

Potter, P.E. 1978. Significance and origin of big rivers. *Journal of Geology*, **86**, 13–33.

Ramírez-Sánchez, E., Hervé, F., Kelm, U. & Sassi, R. 2005. *P–T* conditions of metapelites from metamorphic complexes in Aysen. *Journal of South American Earth Sciences*, **19**, 373–386.

Ramos, V.A. 1984. Patagonia: ¿un continente paleozóico a la deriva? *In: IX Congreso Geológico Argentino, Bariloche, Actas*, **II**, 311–325.

Ramos, V.A. 1989. Andean foothills structures in northern Magellanes Basin, Argentina. *AAPG Bulletin*, **73**, 887–903.

Rapalini, A.E. 1998. Syntectonic magnetization of the mid-Palaeozoic Sierra Grande Formation: further constraints on the tectonic evolution of Patagonia. *Journal of the Geological Society, London*, **155**, 105–114.

Rapela, C.W., Pankhurst, R.J., Casquet, C., Baldo, E., Saavedra, J., Galindo, C. & Fanning, C.M. 1998. The Pampean Orogeny of the southern proto-Andes: Cambrian continental collision in the Sierras de Córdoba. *In:* Pankhurst, R.J. & Rapela, C.W. (eds) *The Proto-Andean Margin of Gondwana*. Geological Society, London, Special Publications, **142**, 181–217.

Rapela, C.W., Pankhurst, R.J., Fanning, C.M. & Grecco, L.E. 2003. Basement evolution of the Sierra de la Ventana Fold Belt: new evidence for Cambrian continental rifting along the southern margin of Gondwana. *Journal of the Geological Society, London*, **160**, 613–628.

Ravikant, V., Bhaskar Rao, Y.J. & Gopalan, K. 2004. Schirmacher Oasis as an extension of the Neoproterozoic East African Orogen into Antarctica: new Sm–Nd isochron age constraints. *Journal of Geology*, **112**, 607–616.

Riccardi, A.C. 1971. Estratigrafía en el oriente de la Bahía de la Lancha, Lago San Martín, Santa Cruz, Argentina. *Revista del Museo de La Plata (nueva serie), Sección Geología*, **VII**, 245–318.

Samson, S.D., D'Lemos, R.S., Blichert-Toft, J. & Vervoort, J. 2003. U–Pb geochronology and Hf–Nd isotope compositions of the oldest Neoproterozoic crust within the Cadomian orogen: new evidence for a unique juvenile crust. *Earth and Planetary Science Letters*, **208**, 165–180.

Sato, A.M., Tickyj, H., Llambías, E.J. & Sato, K. 2000. The Las Matras tonalitic–trondhjemitic pluton, central Argentina: Grenvillian-age constraints, geochemical characteristics, and regional implications. *Journal of South American Earth Sciences*, **13**, 587–610.

Scherer, E., Münker, C. & Mezger, K. 2001. Calibration of the lutetium–hafnium clock. *Science*, **293**, 683–687.

Steenken, A., Wemmer, K., López de Luchi, M., Siegesmund, S. & Pawlig, S. 2004. Crustal provenance and cooling of the basement complexes of the Sierra de San Luis: an insight into the tectonic history of the proto-Andean margin of Gondwana. *Gondwana Research*, **7**, 1171–1195.

Storey, B.C., Pankhurst, R.J. & Johnson, A.C. 1994. The Grenville Province within Antarctica: a test of the SWEAT hypothesis. *Journal of the Geological Society, London*, **151**, 1–4.

Taylor, G.K. & Shaw, J. 1989. The Falkland Islands: new palaeomagnetic data and their origin as a displaced terrane from southern Africa. *In:* Hillhouse, J.W. (ed.) *Deep Structure and Past Kinematics of Accreted Terranes*. Geophysical Monographs, American Geophysical Union, **50**, 59–72.

Thistlewood, L., Leat, P.T., Millar, I.L., Storey, B.C. & Vaughan, A.P.M. 1997. Basement geology and Palaeozoic–Mesozoic mafic dykes from the Cape Meredith Complex, Falkland Islands: a record of repeated intracontinental extension. *Geological Magazine*, **134**, 355–367.

Thomas, R.J., Henjes-Kunst, F. & Jacobs, J. 1998. Pre-lamprophyre mafic dykes of the Cape Meredith Complex, West Falkland. *Geological Magazine*, **135**, 495–500.

Thomson, S.N. & Hervé, F. 2002. New time constraints for the age of metamorphism at the ancestral Pacific Gondwana margin of southern Chile (42–52°S). *Revista Geológica de Chile*, **29**, 255–271.

Varela, R., Dalla Salda, L., Cingolani, C. & Gomez, V. 1991. Estructura, petrología y geocronología del basamento de la región del Limay, Províncias de Río Negro y Neuquén, Argentina. *Revista Geológica de Chile*, **18**, 147–163.

Veizer, J. & Jansen, S.L. 1985. Basement and sedimentary recycling—2: time dimension to global tectonics. *Journal of Geology*, **93**, 625–643.

Vervoort, J.D. & Blichert-Toft, J. 1999. Evolution of the depleted mantle: Hf isotope evidence from juvenile rocks through time. *Geochimica et Cosmochimica Acta*, **63**, 533–556.

Vervoort, J.D. & Patchett, P.J. 1996. Behavior of hafnium and neodymium isotopes in the crust: constraints from Precambrian crustally derived granites. *Geochimica et Cosmochimica Acta*, **60**, 3717–3733.

Vervoort, J.D., Patchett, P.J., Blichert-Toft, J. & Albarède, F. 1999. Relationships between Lu–Hf and Sm–Nd isotopic systems in the global sedimentary system. *Earth and Planetary Science Letters*, **168**, 79–99.

Vervoort, J.D., Patchett, P.J., Albarède, F., Blichert-Toft, J., Rudnick, R. & Downes, H. 2000. Hf–Nd isotopic evolution of the lower crust. *Earth and Planetary Science Letters*, **181**, 115–129.

von Gosen, W. 2003. Thrust tectonics in the North Patagonian Massif (Argentina): implications for a Patagonia plate. *Tectonics*, **22**(1005), 1–13.

Wareham, C.D., Pankhurst, R.J., Thomas, R.J., Storey, B.C., Grantham, G.H., Jacobs, J. & Eglington, B.M. 1998. Pb, Nd, and Sr isotope mapping of Grenville-age crustal provinces in Rodinia. *Journal of Geology*, **106**, 647–659.

Wareham, C.D., Stump, E., Storey, B.C., Millar, I.L. & Riley, T.R. 2001. Petrogenesis of the Cambrian Liv Group, a bimodal volcanic rock suite from the Ross orogen, Transantarctic Mountains. *Geological Society of America Bulletin*, **113**, 360–372.

Williams, I.S. 1998. U–Th–Pb geochronology by ion microprobe. *In:* McKibben, M.A., Shanks, W.C. III & Ridley, W.I. (eds) *Applications of Microanalytical Techniques to Understanding Mineralizing Processes*. Reviews in Economic Geology, **7**, 1–35.

Willner, A.P., Hervé, F. & Massonne, H.-J. 2000. Mineral chemistry and pressure–temperature evolution of two contrasting high-pressure–low-temperature belts in the Chonos Archipelago, southern Chile. *Journal of Petrology*, **41**, 309–330.

Willner, A.P., Glodny, J., Gerya, T.V., Godoy, E. & Massonne, H.-J. 2004a. A counterclockwise *PTt* path of high-pressure/low-temperature rocks from the Coastal Cordillera accretionary complex of south–central Chile: constraints for the earliest stage of subduction mass flow. *Lithos*, **75**, 283–310.

Willner, A.P., Hervé, F., Thomson, S.N. & Masonne, H.-J. 2004b. Converging *P–T* paths of Mesozoic HP–LT metamorphic units (Diego de Almagro

Island, Southern Chile): evidence for juxtaposition during late shortening of an active continental margin. *Mineralogy and Petrology*, **81**, 43–84.

Willner, A.P., Thomson, S.N., Kröner, A., Wartho, J.-A., Wijbrans, J.R. & Hervé, F. 2005. Time markers for the evolution and exhumation history of a Late Palaeozoic paired metamorphic belt in north–central Chile (34°–35°30′S). *Journal of Petrology*, **46**, 1835–1858.

Yoshida, K. 1981. *Estudio geológico del curso superior del río Baker, Aysén, Chile (47°05′ a 47°42′ Lat. S., 72°28′ a 73°15′ Long. W.)*. PhD thesis, Universidad de Chile, Santiago de Chile.

Young, D.N., Zhao, J.-X., Ellis, D.J. & McCulloch, M.T. 1997. Geochemical and Sr–Nd isotopic mapping of source provinces for the Mawson charnockites, East Antarctica: implications for Proterozoic tectonics and Gondwana reconstruction. *Precambrian Research*, **86**, 1–19.

Zhao, J.-X., Ellis, D.J., Kilpatrick, J.A. & McCulloch, M.T. 1997. Geochemical and Sr–Nd isotopic study of charnockites and related rocks in the northern Prince Charles Mountains, East Antarctica: implications for charnockite petrogenesis and Proterozoic crustal evolution. *Precambrian Research*, **81**, 37–66.

Received 14 October 2005; revised typescript accepted 23 March 2006.
Scientific editing by David Peate